

8816 IR

RI 9188

Bureau of Mines Report of Investigations/1988

Horizontal and Vertical Load Transferring Mechanisms in Longwall Roof Supports

By Thomas M. Barczak and David E. Schwemmer



UNITED STATES DEPARTMENT OF THE INTERIOR



Report of Investigations 9188

Horizontal and Vertical Load Transferring Mechanisms in Longwall Roof Supports

By Thomas M. Barczak and David E. Schwemmer

**UNITED STATES DEPARTMENT OF THE INTERIOR
Donald Paul Hodel, Secretary**

**BUREAU OF MINES
T S Ary, Director**

Library of Congress Cataloging in Publication Data:

Barczak, Thomas M.

Horizontal and vertical load transferring mechanisms in longwall roof supports.

(Bureau of Mines report of investigations ; 9188)

Bibliographies.

Supt. of Docs.: I 28.23:9188.

1. Mine roof control. 2. Longwall mining. I. Schwemmer, David E. II. Title. III. Series: Reports of investigations (United States. Bureau of Mines) ; 9188.

TN23.U43

[TN288]

622 s [622'.334]

88-600178

CONTENTS

	<u>Page</u>
Abstract.....	1
Introduction.....	2
Support and strata interactions.....	4
Support reaction and load transfer models.....	6
Full shield model.....	6
Caving shield-lemniscate assembly model.....	6
Leg cylinder model.....	7
Load transfer analysis.....	7
Stiffness determinations.....	7
Shield mechanics.....	9
Full shield responses.....	11
Load distribution.....	14
Implications on shield design and utilization.....	14
Future research.....	15
Conclusions.....	16
Appendix A.--Description of MRS and its capabilities.....	17
Appendix B.--Stiffness test procedures and results.....	18
Appendix C.--Shield mechanics equilibrium analysis.....	23

ILLUSTRATIONS

1. Two-dimensional diagram of longwall shield.....	2
2. Mine roof support optimization plan.....	3
3. Evaluation of a shield in MRS.....	4
4. Axis orientation for shield displacements.....	5
5. Shield boundary conditions and physical interpretations.....	5
6. Load transferring paths in shield supports.....	6
7. Sectioning of shield structure for equilibrium analysis.....	9
8. Frictionless canopy analysis.....	10
9. Analysis of forces at leg joint for frictionless canopy condition.....	10
10. Restrained canopy and base analysis.....	10
11. Face-to-waste strata movement analysis.....	10
12. Analysis of forces at leg joint for face-to-waste strata movement.....	11
13. Instrumented pin.....	12
14. Pin translational freedom.....	13
15. Change in leg stiffness as a function of leg staging.....	15
B-1. Displacement patterns for stiffness tests.....	18
B-2. Example of stiffness determinations in MRS.....	18
B-3. Caving shield-lemniscate assembly stiffness test conditions.....	19
B-4. Example of load-displacement relationship for caving shield-lemniscate assembly.....	19
B-5. VH caving shield-lemniscate assembly test results.....	20
B-6. HV caving shield-lemniscate assembly test results.....	20
B-7. Unconstrained full shield stiffness results.....	21
B-8. Constrained full shield stiffness results.....	22

TABLES

	<u>Page</u>
1. Caving shield-lemniscate assembly stiffness coefficients.....	8
2. Unconstrained full shield stiffness coefficients.....	8
3. Constrained full shield stiffness coefficients.....	8
4. Load transfer mechanics full shield response predicitions.....	12
5. Full shield response predictions for constrained shield condition.....	13
6. Frictionless canopy full shield response predictions.....	14
7. Load distribution for unconstrained and constrained shield conditions.....	14

UNIT OF MEASURE ABBREVIATIONS USED IN THIS REPORT

ft	foot	kip/in	kip per inch
in	inch	pct	percent
in ²	square inch	psi	pound per square inch

HORIZONTAL AND VERTICAL LOAD TRANSFERRING MECHANISMS IN LONGWALL ROOF SUPPORTS

By Thomas M. Barczak¹ and David E. Schwemmer²

ABSTRACT

This report describes a study that examined load transfer mechanics in longwall shield supports as part of the Bureau of Mines research program to optimize support design and utilization. The objectives of this study were to determine the contribution of the leg cylinders and the caving shield-lemniscate assembly towards full shield vertical and horizontal load resistance capability and to determine how the interaction of these members affect overall shield response. Load-displacement characteristics of the leg cylinders and the caving shield-lemniscate assembly, independent of the full shield, were evaluated from controlled displacement tests in the Bureau's mine roof simulator and responses were compared with full shield responses to identify load transfer mechanics. It is concluded from this research that the participation of the caving shield-lemniscate assembly significantly affects the response of the shield support. It is likely that the caving shield-lemniscate assembly is not participating fully in current shield designs because of translational freedom in the numerous pin joints. It is also concluded that the shield will respond differently to different boundary conditions resulting from interaction with the strata. This report describes load transfer mechanics of shield supports and the implication of these research findings on shield design and utilization.

¹Research physicist, Pittsburgh Research Center, Bureau of Mines, Pittsburgh, PA.

²Structural engineer, Boeing Services International.

INTRODUCTION

Extraction of coal in underground mining creates an opening that must be stabilized to permit safe mining operations. In longwall mining, stability of the face area is provided by the powered roof support system. A series of support structures (longwall shields) are employed along the face to provide a temporary working space for personnel and machinery for extraction of the coal. The shields must function to resist relative motion between the roof and floor strata as the strata tries to reestablish a stable configuration. More specifically, the roof support must function to (1) control vertical (roof-to-floor) convergence and (2) maintain stability against horizontal displacements resulting from strata activity.

A two-dimensional diagram of a two-legged longwall shield is shown in figure 1. A basic operation of the shield is described by Peng.³ To facilitate a study of load transfer mechanics, the shield will be addressed in four components: (1) canopy or roof beam, (2) caving shield-lemniscate assembly, (3) leg cylinders, and (4) base or floor beam. The canopy and base serve as an interface between the roof and floor strata. Loads applied to the canopy by activity of the roof strata must be transmitted through the leg cylinders and/or caving shield-lemniscate assembly to the base to provide equilibrium. How these loads are transmitted through the support structure is an important consideration in support design. An understanding of the load transfer mechanics is necessary to properly size and eventually optimize support components and to understand the reaction of the support to strata behavior.

This research is part of the Bureau of Mines research program to optimize mine roof support systems. Optimization can be considered in terms of (1) support

selection and (2) support design, as illustrated in the optimization plan shown in figure 2. This study concentrates on evaluation of support mechanics and interaction of the support with the strata. The primary contributions of this study toward the optimization goals is the identification of load transferring mechanisms within the support structure and the response of the support to boundary conditions (vertical and horizontal displacements) imposed by the strata. More specifically, the objectives of this study are (1) to quantify the stiffness of the full shield, the caving shield-lemniscate assembly, and the leg cylinders; (2) analytically evaluate the interaction of the caving shield-lemniscate assembly with that of full shield responses; and (3) suggest implications of these findings relative to shield utilization and design. Influential parameters investigated in this research project were shield height effects, horizontal translational freedom (constrained versus unconstrained initial shield conditions at shield setting), and various restraints on the canopy and base (boundary conditions).

These tasks were accomplished from controlled testing of a full-scale longwall support in the Bureau's mine roof simulator (MRS). A description of the MRS and its capabilities is provided in appendix A. Figure 3 shows a shield undergoing evaluation in the simulator.

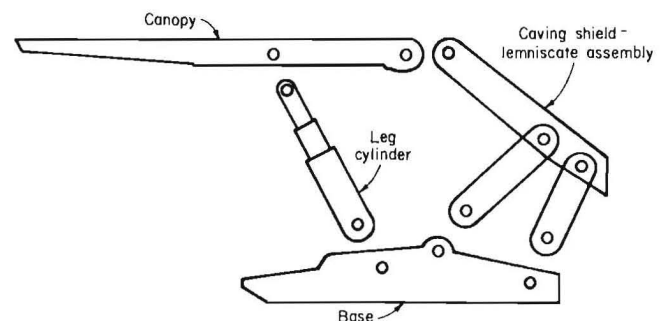


FIGURE 1.—Two-dimensional diagram of longwall shield.

³Peng, S. S. Longwall Mining. Wiley, 1984, pp. 150-182.

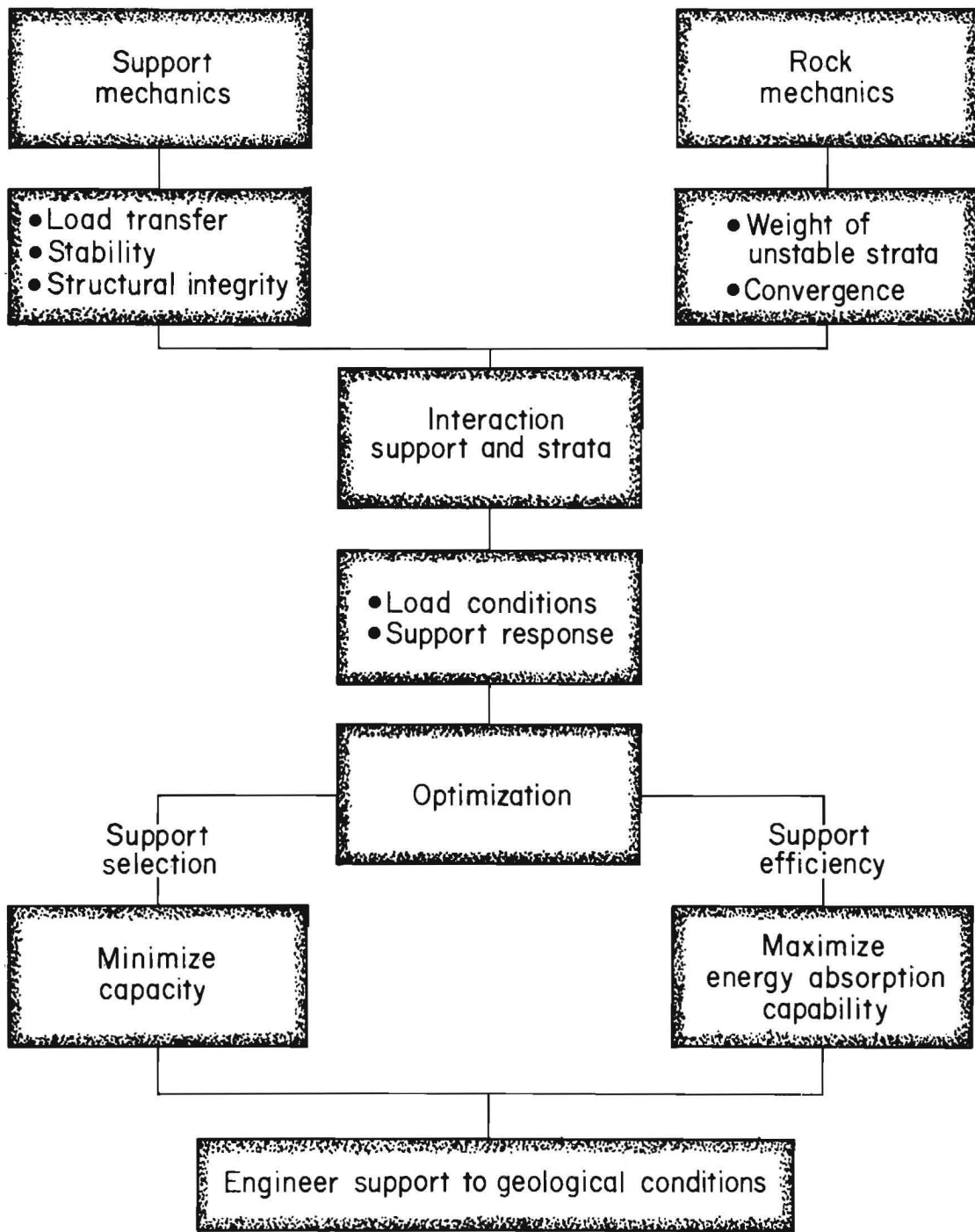


FIGURE 2.—Mine roof support optimization plan.

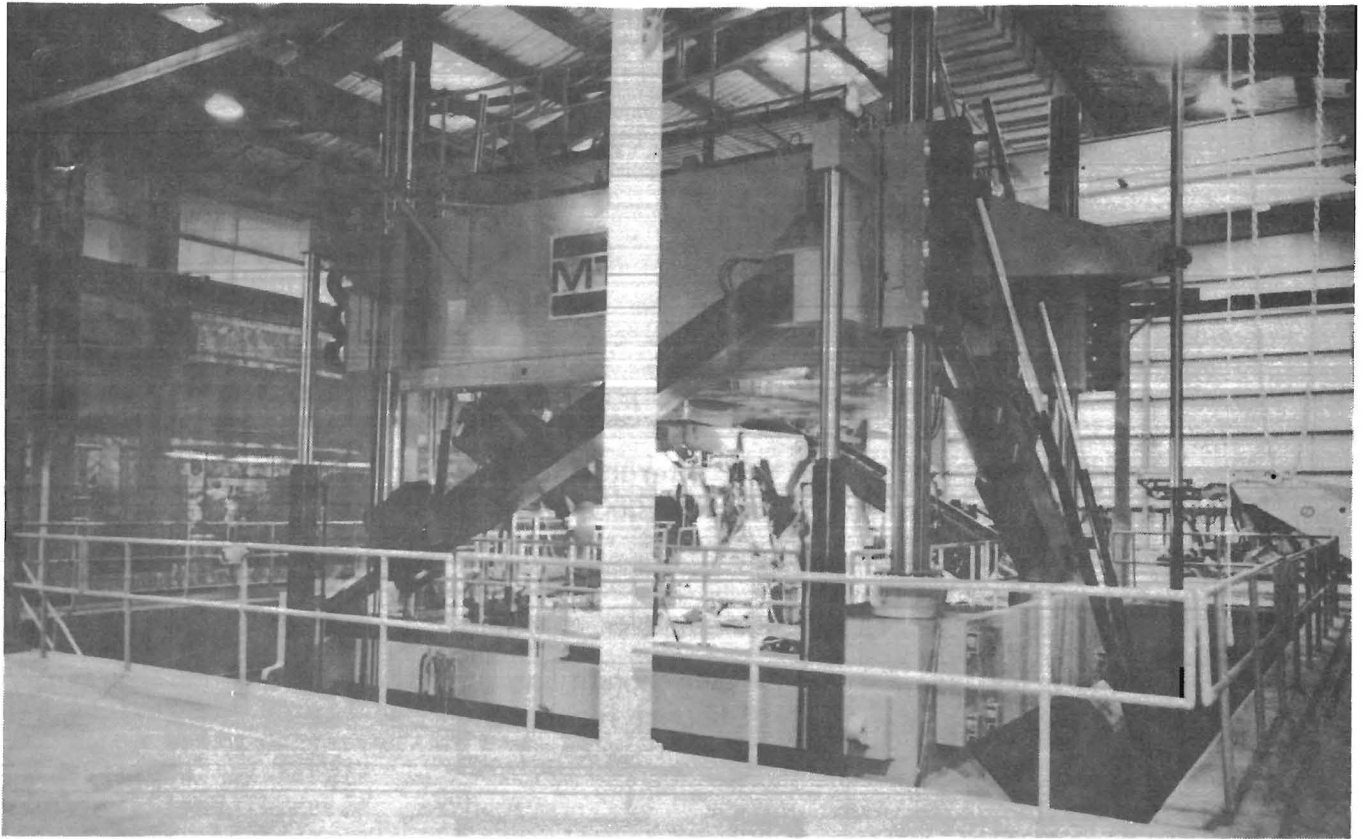


FIGURE 3.--Evaluation of a shield in MRS.

Previous research by the Bureau has developed techniques to evaluate shield responses by development of mathematical models to assess shield stiffness.⁴ This study utilizes these techniques to investigate load transfer mechanics in a shield support. This load transfer mechanics research is considered a first in this field because of the unique capabilities of the MRS to provide controlled horizontal and vertical displacements to full-scale shield supports.

The potential benefits of research to optimize longwall supports are a reduction in support costs and more effective ground control, leading to more productive and safer working environments. These benefits will be realized by selecting supports that are more compatible with the conditions in which they are to be employed and by design of a more uniformly and fully stressed support structure.

SUPPORT AND STRATA INTERACTIONS

The primary function of the support is to maintain stability against vertical and horizontal displacements resulting

from strata activity. As the canopy and base interface with the roof and floor strata, shield displacements occur from the relative motion between the canopy and base of the support structure. Figure 4 depicts an axis orientation for diagrammatically depicting shield displacement directions. Vertical displacements are in reference to the separations between the canopy and base, while horizontal displacements refer to horizontal

⁴Barczak, T. M., and W. S. Burton. Assessment of Longwall Roof Behavior and Support Loading by Linear Elastic Modeling of the Support Structure. BuMines RI 9081, 1987, 7 pp.

Barczak, T. M. Rigid-Body and Elastic Solutions to Shield Mechanics. BuMines RI 9144, 1987, 20 pp.

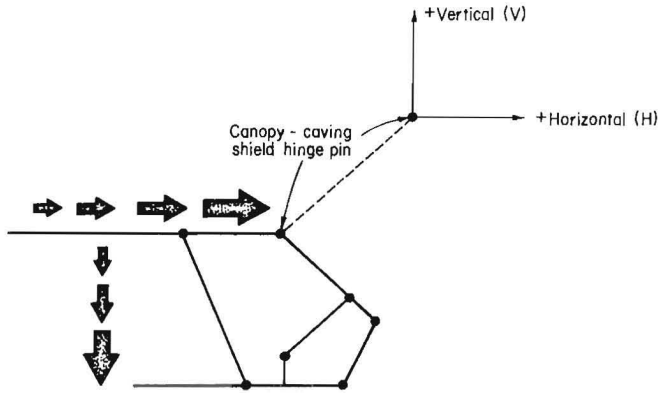


FIGURE 4.--Axis orientation for shield displacements.

translation of the canopy relative to the base.

The shield, once set against the roof and in an equilibrium configuration, may be subjected to combinations of vertical and horizontal displacements (or forces) during operation. Positive, zero, or negative directions can occur for each displacement, providing a total of nine different combinations of horizontal and vertical displacement. Of these, only three combinations are considered relevant for typical mining operations. With the axis orientation depicted in figure 4, these three combinations are a negative vertical (roof-to-floor) displacement; in conjunction with a positive (face-to-waste), zero (pure vertical convergence), or negative (waste-to-face) horizontal displacement of the canopy relative to the base.

A physical interpretation of these displacement profiles is described in terms of boundary conditions existing between the support and its environment as depicted in figure 5.

1. Restrained canopy and base.--Pure vertical displacement is described as a restrained canopy and base boundary condition where there is no horizontal translation of the canopy relative to the base. This is likely to occur when there is roof-to-floor strata convergence and when the canopy and base are restrained, either by frictional forces at the strata interface or by protrusions in the strata, to prevent horizontal translation of the canopy by internal shield forces created from horizontal components of the leg forces.

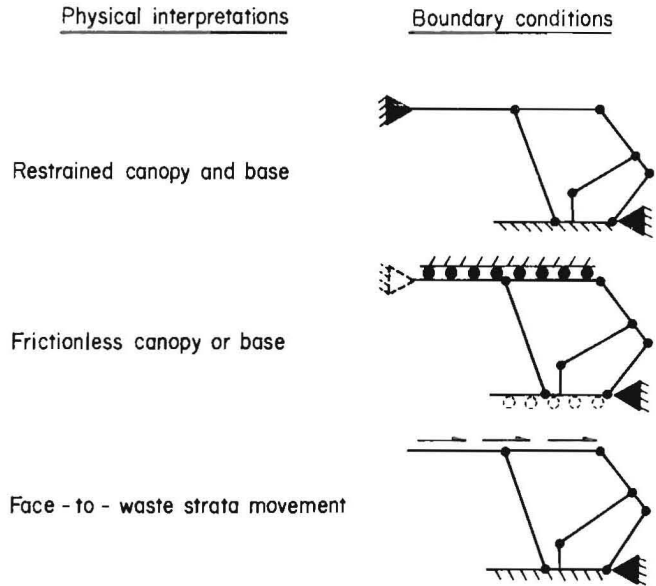


FIGURE 5.--Shield boundary conditions and physical interpretations.

2. Frictionless canopy or base.--A negative horizontal displacement condition exists when the canopy is translated horizontally toward the face relative to the base. This will occur by action of the horizontal component of the leg forces when there is insufficient friction between the support and the interfacing strata to prevent this translation. This condition will develop when the base is restrained and the canopy is translated towards the face, or, if the canopy was restrained and the base slid under loading towards the gob. This behavior is most likely to occur in friable roof or soft bottom conditions. Negative horizontal displacement of the canopy towards the face can also occur as a result of gob loading on the caving shield, again when there is insufficient friction between the support and the strata or restraint by the caving shield-lemniscate assembly to prevent this translation.

3. Face-to-waste strata movement.--Translation of the canopy toward the gob (positive horizontal translation) occurs when there is face-to-waste movement of the strata and there is sufficient friction or restraint between the canopy and roof to translate this displacement to the support structure.

SUPPORT REACTION AND LOAD TRANSFER MODELS

This section describes the development of analytical models used to evaluate support behavior. To evaluate load transfer mechanics within the support structure, it is necessary to determine the response of support components (assemblies) as well as that of the full shield. As can be seen in figure 6, there are two load transferring paths between the canopy and base of a typical two-leg longwall shield: one is through the leg cylinder and the other is through the caving shield-lemniscate assembly. Therefore, three models are developed: (1) full shield model, (2) caving shield-lemniscate model, and (3) leg cylinder model. The full shield and caving shield-lemniscate model describe the elastic response of these components to applied vertical and horizontal displacements. These models employ computation of component stiffness from load-displacement relationships derived in the MRS. The leg model computes leg forces from measured hydraulic pressures.

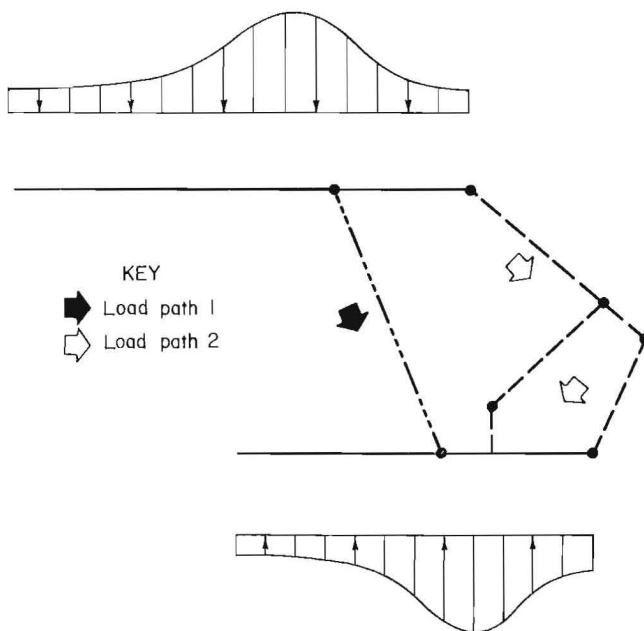


FIGURE 6.—Load transferring paths in shield supports.

FULL SHIELD MODEL

The reaction of the support to applied vertical and horizontal displacements is described in the following two-dimensional linear elastic analytical model:⁵

$$VF_{sh} = K1_{sh} * V_{sh} + K2_{sh} * H_{sh}, \quad (1)$$

and

$$HF_{sh} = K3_{sh} * V_{sh} + K4_{sh} * H_{sh}, \quad (2)$$

where VF_{sh} = vertical shield reaction,

HF_{sh} = horizontal shield reaction,

V_{sh} = vertical displacement (of canopy),

H_{sh} = horizontal displacement (of canopy),

and

$K1_{sh}, K2_{sh}, K3_{sh}, K4_{sh}$ = full shield stiffness coefficients.

CAVING SHIELD-LEMNISCATE ASSEMBLY MODEL

The approach previously described to model the full shield response can also be utilized to describe the response of the caving shield-lemniscate assembly to applied displacements:

$$VF_c = K1_c * V_c + K2_c * H_c, \quad (3)$$

$$HV_c = K3_c * V_c + K4_c * H_c, \quad (4)$$

where VF_c = vertical reaction of caving shield-lemniscate assembly,

HF_c = horizontal reaction of caving shield-lemniscate assembly,

V_c = vertical displacement of caving shield,

⁵Works cited in footnote 4.

H_c = horizontal displacement of
caving shield,

and

$K1_c, K2_c,$
 $K3_c, K4_c$ = caving shield-lemniscate
assembly stiffness
coefficients.

LEG CYLINDER MODEL

Attempts were made to model the leg cylinder as a single degree of freedom axial member where vertical and horizontal shield (canopy) displacements produce axial loads in proportion to the stiffness of the leg cylinder. However, it was discovered that the leg stiffness was a function of the extension of the leg stages in the two-stage leg specimen. Because controlling the leg extensions proved to be difficult, quantification of leg stiffness characteristics were considered beyond the scope of this project and will be investigated in future studies.

Alternatively, since leg pressure is relatively easy to measure and since the effective leg cylinder area was found to

remain constant, loading in the legs was determined by measurement of leg pressures. Horizontal and vertical components of the leg force were then determined from the geometric relationship of the leg orientation for specific shield configurations.

$$L = P * A, \quad (5)$$

where L = leg force,

P = measured leg pressure,

and A = bore area of leg cylinder.

$$L_v = L * \cos \theta, \quad (6)$$

$$L_h = L * \sin \theta, \quad (7)$$

where L_v = vertical component of leg force,

L_h = horizontal component of leg force,

and θ = angle between leg cylinder and normal to plane of canopy.

LOAD TRANSFER ANALYSIS

The development of load transfer mechanics is pursued as follows. First, the stiffness characteristics of the caving shield-lemniscate assembly and the full shield are determined in accordance with the models presented in the previous section. Then an assessment of shield mechanics is made by evaluation of the interaction and contribution of the leg cylinders and caving shield-lemniscate assembly towards full shield responses. This is done by comparison of full shield response predictions from the summation of leg cylinder and caving shield-lemniscate assembly reactions to full shield responses predicted from the full shield analytical model. Finally, verification of these full shield predictions are made by comparison of the analytical model predictions with measured (MRS) full shield physical responses.

STIFFNESS DETERMINATIONS

The stiffness of the caving shield-lemniscate assembly itself (independent of the full shield), and of the full shield have been determined from controlled tests in the MRS for combinations of horizontal and vertical displacements. Two displacement patterns were applied: one where the vertical displacement is applied first (designated as VH tests), and the other where the horizontal displacement is applied first (designated as HV tests). Test procedures and results are documented in appendix B.

Representative stiffnesses are shown in tables 1 through 3. Caving shield-lemniscate assembly test results (stiffness) are summarized in table 1. Full shield stiffnesses are shown in tables 2 and 3. Table 2 represents a horizontally

TABLE 1. - Caving shield-lemniscate assembly stiffness coefficient, kips per inch

Displacement pattern at height, in	$K1_c$	$K2_c$	$K3_c$	$K4_c$
Vertical-horizontal:				
87.5.....	6	115	15	365
78.0.....	0	75	0	510
68.0.....	0	85	15	550
56.0.....	0	95	15	680
Horizontal-vertical:				
87.5.....	30	90	120	325
78.0.....	10	70	25	400
68.0.....	25	75	55	470
56.0.....	30	80	100	565

TABLE 2. - Unconstrained full shield stiffness coefficients, kips per inch

Displacement pattern at height, in	$K1_{sh}$	$K2_{sh}$	$K3_{sh}$	$K4_{sh}$
Vertical:				
87.5.....	730	190	245	195
78.0.....	740	305	275	280
68.0.....	800	370	325	305
56.0.....	910	565	495	420
Horizontal:				
87.5.....	655	225	205	185
78.0.....	770	290	300	250
68.0.....	820	380	306	320
56.0.....	945	535	500	330

TABLE 3. - Constrained full shield stiffness coefficients, kips per inch

Displacement pattern at height, in	$K1_{sh}$	$K2_{sh}$	$K3_{sh}$	$K4_{sh}$
Vertical:				
87.5.....	710	275	255	435
78.0.....	730	255	415	295
68.0.....	690	245	300	670
56.0.....	875	500	485	945
Horizontal:				
87.5.....	615	285	290	315
78.0.....	650	280	260	265
68.0.....	705	285	330	645
56.0.....	930	495	465	930

unconstrained shield (canopy-base) configuration and table 3 is for a horizontally constrained shield (canopy-base) configuration prior to load application. Again, reference to horizontal constraint is intended to indicate the degree of translational freedom present in the shield at loading due to pin and/or clevis fabrication and installation tolerances in the numerous joints in the shield structure. Effective leg cylinder area was experimentally determined from controlled MRS displacement tests of the leg cylinder independent of the full shield. Bore area was computed as the ratio of the MRS force to measured leg pressure. Conclusions drawn from these tests follows.

Caving Shield-Lemniscate Assembly

1. The caving shield-lemniscate assembly has virtually no capacity to resist vertical displacements, as indicated by the lack of vertical stiffness ($K1_c = 0$) in this assembly. This suggests that for vertical loading, all of the load is transferred from the canopy to the base by the leg cylinders.

2. Some vertical load capacity is generated in the caving shield-lemniscate assembly by horizontal displacements ($K2_c$ coefficient), but this capacity is less than 15 pct of the leg cylinder capacity. Hence, the leg cylinder continues to be the primary load transfer mechanism for vertical shield loading.

3. The caving shield has considerable capacity to resist horizontal displacements (large $K4_c$ stiffness coefficient). For conditions resulting in horizontal translations of the canopy, it can be the primary load transferring mechanism.

4. Vertical displacements generally produce insignificant horizontal reactions by the caving shield-lemniscate assembly as evidenced by the near zero $K3_c$ stiffness coefficient. However, when the vertical displacement is preceded by a horizontal displacement, some vertical

stiffness is generated in the caving shield-lemniscate assembly providing some horizontal reaction to vertical displacement. This observation indicates a caving shield-lemniscate assembly response dependency on the sequence of the vertical and horizontal displacement applications.

Leg Cylinders

5. The contribution of the leg cylinder in resisting vertical and horizontal displacements (loading) is influenced by the orientation of the leg cylinder, which changes with shield height. As the height increases, the leg cylinder is oriented in a more vertical position, producing less of a horizontal component, and thereby reducing that component of the leg force available to resist horizontal loading, while increasing its capability to resist vertical loading.

6. Effective leg cylinder area, determined from the slope of (MRS) force versus leg pressure plots, was found to be nearly constant at 69 to 70 in² for any leg length. This suggests that determination of leg force from pressure computations is acceptable.

Full Shield Stiffness

7. Full shield stiffness, both vertical and horizontal, increases with reduction in shield height.

8. Overall, the unconstrained shield is much stiffer vertically than horizontally ($K1_{sh} = K2_{sh} > K3_{sh} + K4_{sh}$), for equal vertical and horizontal displacements. When constrained, the horizontal full shield stiffness approaches the vertical stiffness at the high heights and exceeds the vertical stiffness at the low heights.

9. It is seen from comparison of tables 2 and 3, that the shield is stiffer horizontally when constrained than unconstrained ($K4_{sh} \text{ constrained} > K4_{sh} \text{ unconstrained}$).

SHIELD MECHANICS

Contribution of the leg cylinders and the caving shield-lemniscate assembly to full shield vertical and horizontal load response is dependent upon the interaction of these components. To evaluate this interaction, an analysis of shield mechanics is required.

Considering the overall shield geometry, it is possible to section the structure into three areas for analysis of static equilibrium. Figure 7 designates these sections as the canopy, leg, and caving shield-lemniscate-base assembly. Further, the canopy is substructured into joints and connecting members so as to facilitate examination of load transfer within the shield structure. Full canopy and base contact conditions are assumed, with the distributed load concentrated at the joints for simplicity of load transfer examination.

Figures 8 through 11 depict internal shield forces and moments for the three boundary and displacement conditions described in the "Support and Strata Interactions" section. Figure 8 depicts the frictionless canopy condition producing a horizontal displacement of the canopy

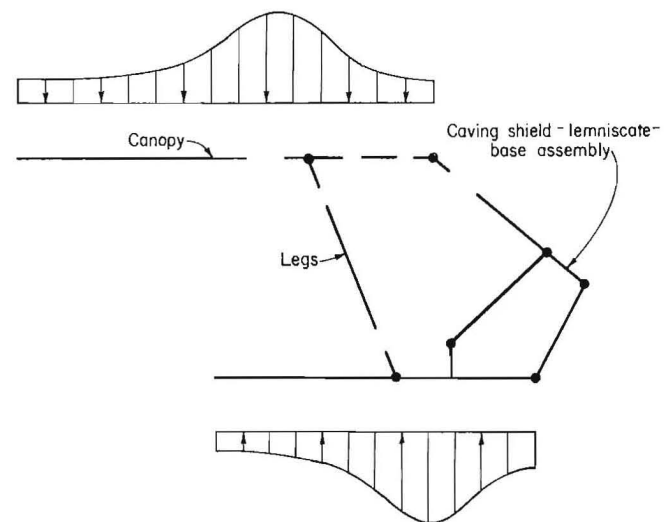


FIGURE 7.—Sectioning of shield structure for equilibrium analysis.

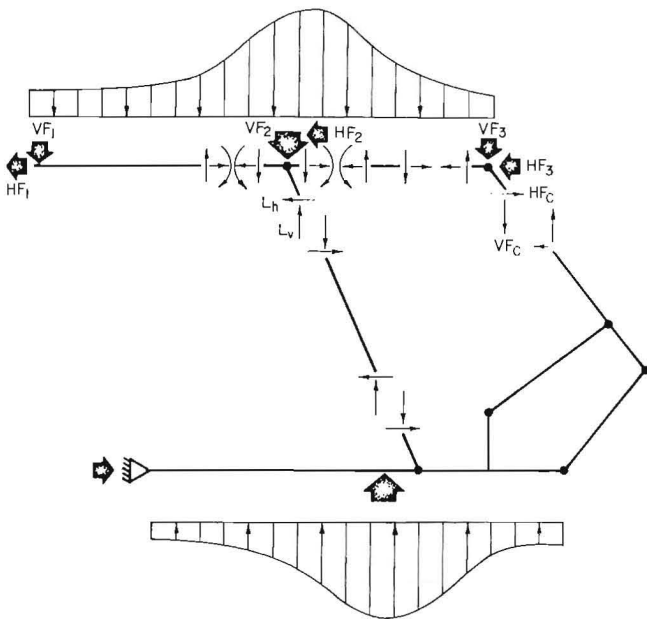


FIGURE 8.—Frictionless canopy analysis.

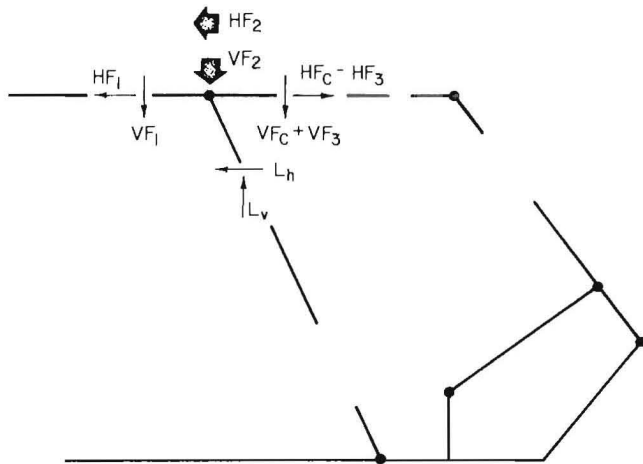


FIGURE 9.—Analysis of forces at leg joint for frictionless canopy condition.

towards the face, figure 10 represents a restrained canopy and base condition with no horizontal translation of the canopy, and figure 11 describes face-to-waste canopy translation.

Appendix C documents the equilibrium requirements for these conditions. The following is summary of results and conclusions drawn from this analysis.

1. Frictionless canopy analysis (fig. 8).—The forward motion of the canopy is resisted by the caving shield-lemniscate assembly, which produces a downward

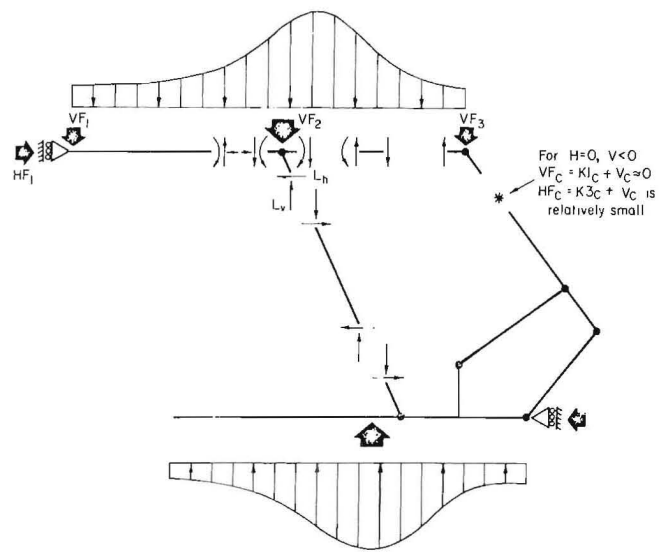


FIGURE 10.—Restrained canopy and base analysis.

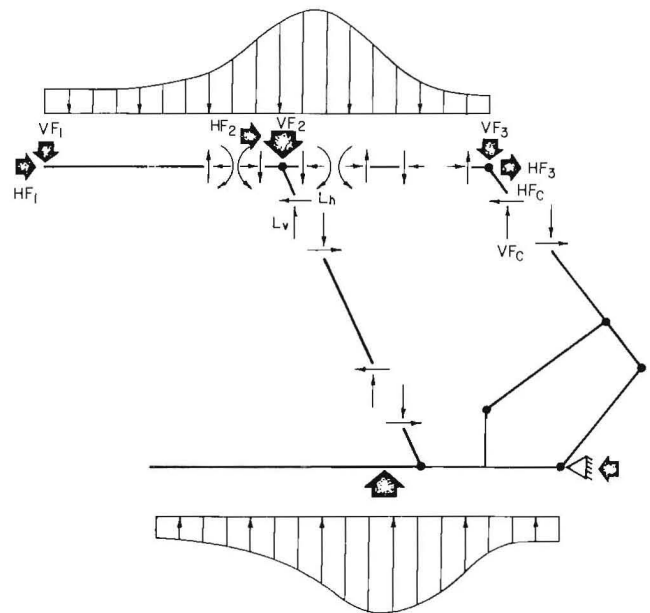


FIGURE 11.—Face-to-waste strata movement analysis.

vertical reaction at the canopy hinge pin. This force is equal to the force generated in the caving shield-lemniscate assembly (V_{F_c}) as a result of the horizontal displacement. From analysis of forces at the leg joint (fig. 9), it is seen that this force counteracts the leg force, thereby reducing the vertical capacity of the support. Similarly, it is seen that a horizontal reaction of the caving shield-lemniscate assembly (H_{F_c}) in response to applied horizontal shield displacements, also acts to counteract

the horizontal component of the leg force and reduce the horizontal load capacity of the shield.

2. Restrained canopy and base (fig. 10).--When the canopy and base are both restrained such that there is no horizontal translation of the canopy, horizontal reactions in the caving shield-lemniscate assembly are not developed. It is also known from previous discussions that the caving shield-lemniscate assembly has virtually no capacity to resist vertical displacements. Thus, the caving shield-lemniscate assembly for this boundary condition does not contribute to the vertical or horizontal capacity of the full shield. In a restrained (canopy and base) condition, the response of the shield is controlled by the behavior of the leg cylinder.

3. Face-to-waste strata movement (fig. 11).--An upward vertical force is produced at the caving shield hinge pin as the caving shield-lemniscate assembly resists the face-to-waste displacement of the canopy. From analysis of forces at the leg joint (fig. 12), it is seen that this force acts in the same direction as the leg force, thereby increasing the vertical capacity of the support. The magnitude of this force (VF_C) is determined from equation 3. Similarly, it is seen that the horizontal reaction of the caving shield-lemniscate assembly (HF_C) to vertical and horizontal displacements also acts to increase the horizontal load capacity of the shield.

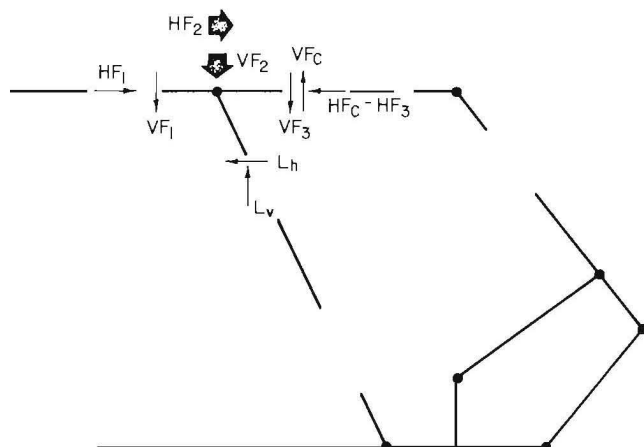


FIGURE 12.--Analysis of forces at leg joint for face-to-waste strata movement.

In summary, the reaction of the caving shield-lemniscate assembly influences vertical and horizontal support resistance. For face-to-waste shield displacements, vertical and horizontal shield resistance is increased, while the vertical and horizontal shield resistance is reduced by the response of the caving shield-lemniscate assembly when the canopy is displaced toward the face. The influence of the caving shield-lemniscate assembly on overall shield response is described in equations 8 through 11, using the nomenclature established in the development of models in the preceding section.

1. Horizontal displacement towards face:

$$HF_{sh} = HF_C - L_h, \quad (8)$$

$$VF_{sh} = L_v - VF_C, \quad (9)$$

2. Horizontal displacement towards gob:

$$HF_{sh} = L_h + HF_C, \quad (10)$$

$$VF_{sh} = L_v + VF_C, \quad (11)$$

Because the horizontal stiffness of the caving shield-lemniscate assembly is much larger than its vertical stiffness ($K1_C + K2_C \ll K3_C + K4_C$, table 1), the action of the caving shield-lemniscate assembly will have a much larger influence on horizontal shield resistance (response) than vertical shield resistance (response).

FULL SHIELD RESPONSES

Example 1--Roof-to-Floor and Face-to-Waste Displacement Profile

Using leg forces determined from leg pressure measurements and caving shield-lemniscate assembly reaction forces determined from equations 3 and 4 with the stiffness data provided in table 1, full shield responses are predicted from the summation of the leg forces and caving shield reactions as indicated in equations 10 and 11. As shown in table 4, these results are compared with full

TABLE 4. - Load transfer mechanics full shield response predictions, kips

Designated height.....in..	87.5		78.0		68.0		56.0	
	Horz	Vert	Horz	Vert	Horz	Vert	Horz	Vert
Component responses:								
Leg cylinders.....	120	370	133	348	126	283	137	220
Caving shield-lemniscate assembly.....	152	48	204	30	141	21	104	14
Full shield responses:								
Legs-caving shield assembly.....	272	418	337	378	267	304	241	234
Full shield model.....	176	368	222	418	157	292	137	221
MRS measurements.....	134	370	188	417	136	290	159	219

shield responses predicted from the full shield stiffness model (equations 1 and 2) for an unconstrained shield configuration prior to setting. These results are also compared with measured MRS force reactions as verification of full shield responses.

As shown in table 4, vertical shield responses predicted from load transfer in the legs and caving shield-lemniscate assembly are predicted accurately (within 10 pct), but the actual full shield

horizontal resistance was considerably less than that predicted by the legs and caving shield-lemniscate assembly interaction. This implies that the participation of the caving shield-lemniscate assembly differed from that inferred from the displacements imposed on the canopy.

To evaluate the load transfer between the canopy and the caving shield, the canopy-caving shield hinge pin was replaced with a load-sensing instrumented pin as shown in figure 13. This pin is

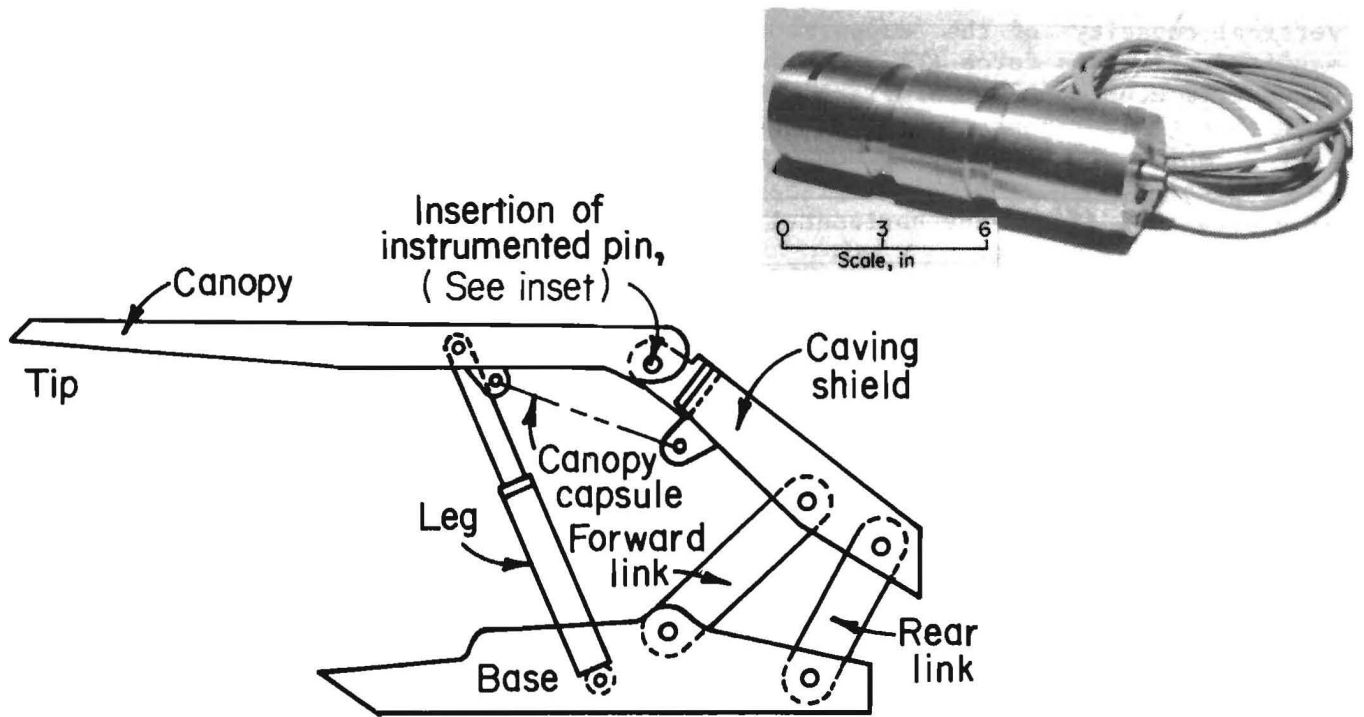


FIGURE 13.-Instrumented pin.

strain gaged internally on two orthogonal axis and oriented in the canopy-caving shield hinge to sense both vertical and horizontal load reactions at this joint. Test results with the instrumented pin revealed low pin activity for unconstrained shield conditions. This low pin activity (small forces) suggested that the displacements applied to the canopy were not being fully transferred to the caving shield-lemniscate assembly. A probable reason for this is translational freedom in the pin joints. It was concluded that the accumulation of pin translational freedom (influenced by degree of shield constraint) prevents the caving shield-lemniscate assembly from developing its full stiffness potential, as was realized when the tests were conducted separately on this assembly where displacements were sufficient to overcome pin freedom.

As shown in table 5, once the pin translational freedom is removed and the caving shield-lemniscate is participating, the full shield predictions are much better. An extensive investigation of the influence of setting conditions on pin translational freedom was not made, but it appears that as long as the canopy and base are not constrained (beyond strata friction), freedom in the pin joints is likely to be sufficient to significantly limit the contribution of the caving shield-lemniscate assembly towards shield responses to subsequent

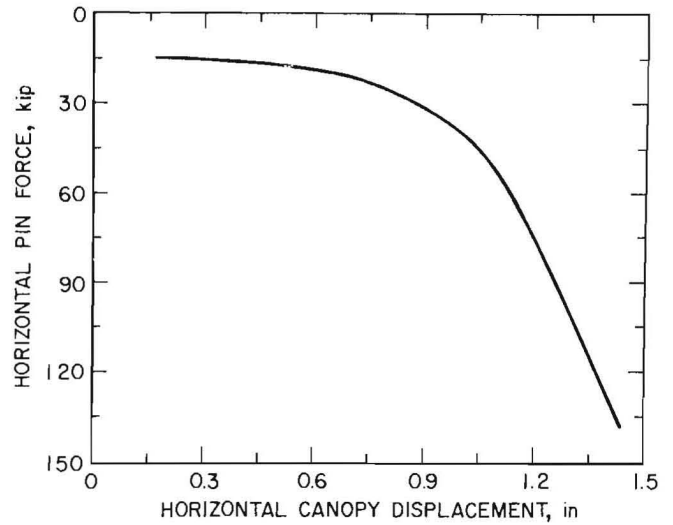


FIGURE 14.—Pin translational freedom.

strata activity (shield displacements). For example, at the higher operating heights, nearly 0.8 in of pin translational freedom was discovered for the particular shield tested in this study. This can be seen in figure 14 by observation of the low pin forces for the first 0.8 in of displacement, followed by a significant (linear) load increase. Hence the difference in full shield stiffness (comparison of tables 2 and 3), is attributable to pin translational freedom. Because the caving shield has virtually no vertical stiffness, the full shield vertical stiffness (capacity) is not significantly affected by the pin translational freedom.

TABLE 5. - Full shield response predictions for constrained shield condition, kips

Designated height.....in..	87.5		78.0		68.0		56.0	
	Horz	Vert	Horz	Vert	Horz	Vert	Horz	Vert
Leg cylinders.....	65	206	70	182	68	152	67	108
Caving shield-lemniscate assembly:								
Model predicitions.....	144	48	102	18	87	16	87	19
Instrumented pin.....	140	55	70	15	76	19	57	17
Full shield responses:								
Legs-caving shield assembly.....	209	254	172	200	155	168	154	127
Legs-instrumented pins..	205	261	140	197	144	171	124	125
Full shield model.....	182	270	142	197	133	165	120	115
MRS measurements.....	205	265	143	197	155	179	130	126

Example 2--Frictionless Canopy Simulation

A frictionless canopy condition was simulated in the MRS by imposing a vertical (roof-to-floor) displacement on the shield while controlling the MRS horizontal force to zero. The horizontal components of the leg forces displace the canopy towards the face until stability is provided by caving shield-lemniscate assembly restraint. As indicated in equations 8 and 9, when the canopy is displaced towards the face, the caving shield-lemniscate assembly forces oppose the leg reactions, requiring the leg forces to equilibrate the sum of both the caving shield-lemniscate assembly forces and external shield forces. This response was verified from the test results for a 87.5-in shield height as shown in table 6. Because the full shield and caving shield-lemniscate assembly stiffnesses were determined for face-to-waste horizontal displacements, the instrumented pin forces and MRS forces are used for comparisons in table 6.

LOAD DISTRIBUTION

As indicated in the previous analysis, the distribution of load between the leg cylinders and the caving shield-lemniscate assembly depends upon the relative displacement and stiffness of these components. Using instrumented canopy-caving shield hinge pin and leg pressure measurements, the distribution of load for equal vertical and horizontal displacements is shown for unconstrained

TABLE 6. - Frictionless canopy full shield response predictions, kips

Shield component(s)	Horz	Vert
Leg cylinders.....	228	723
Caving shield-lemniscate assembly (instrumented pins)	240	23
Full shield responses:		
Legs-instrumented pins.....	12	700
MRS measurements.....	6	723

TABLE 7. - Load distribution for unconstrained and constrained shield conditions

Height, in	Horizontal force, pct		Vertical force, pct	
	Legs	Caving shield assembly	Legs	Caving shield assembly
UNCONSTRAINED				
87.5.....	90	10	100	0
78.0.....	97	3	99	1
68.0.....	98	2	98	2
56.0.....	95	5	99	1
CONSTRAINED				
87.5.....	32	68	79	21
78.0.....	50	50	92	8
68.0.....	46	54	90	10
56.0.....	55	45	86	14

and constrained shield conditions (table 7). Again, it is seen that the participation of the caving shield-lemniscate assembly is significantly reduced by translational freedom in the pin joints when the shield is unconstrained during setting.

IMPLICATIONS ON SHIELD DESIGN AND UTILIZATION

Several fundamental implications on shield design and utilization are evident from these studies of load transfer mechanics.

o As indicated in these studies, considerable pin translational freedom is thought to exist as the summation of the pin and/or clevis tolerances in the numerous joints of current shield designs. It is apparent that performance of the support would be improved if this pin freedom was eliminated. One way to

reduce pin freedom is to provide closer tolerances and more compatible material properties between pins and adjoining clevises. From an operational viewpoint, it may be possible to reduce pin freedom by advancing the shield while in contact with the roof. Pin freedom under actual underground setting conditions was not evaluated in this study.

o The caving shield-lemniscate assembly has sufficient horizontal stiffness, assuming pin freedom is removed, to

provide stability against horizontal shield displacements (loading). This implies that the leg cylinder could be mounted nearly vertical instead of the inclined orientation currently utilized in shield designs. A near vertical leg orientation is more efficient because the full leg force, instead of just the vertical component, can be applied to vertical support resistance.

o Vertical leg orientations are also advantageous from a shield mechanics viewpoint. Current shield designs react both a vertical and horizontal force to vertical displacements and both a horizontal and vertical force to horizontal displacements. This response is the result of the leg being oriented at an

angle other than vertical, where horizontal components of the leg force produce internal forces, which produce shield reactions in directions other than the direction of applied displacements (loading). This is an indication of an inefficient design since stresses in the support structure are developed from the mechanics of the shield and not the activity of the strata.

o The caving shield-lemniscate assembly is necessary in current two-leg shield designs to provide horizontal stability to the support structure in conditions where the canopy or base is likely to slide along the roof or floor interface.

FUTURE RESEARCH

Overall, the stiffness characteristics of the caving shield-lemniscate assembly and the full shield provide reasonable indications of actual shield behavior and load transfer mechanics. However, there are some discrepancies in the general trends observed during this initial study that need further investigation. It appears that inconsistencies in full shield behavior may be largely attributable to changes in leg stiffnesses, as a result of staging of the leg cylinder extensions as shown in figure 15. Future studies are needed to quantify this behavior.

It is also speculated that pin friction is largely responsible for inconsistencies in the caving shield-lemniscate assembly behavior. Future efforts will be directed to quantify the impact of pin friction on overall shield performance and load transfer mechanics.

While this study concentrated on basic load transferring mechanisms between the canopy and base, future studies should also evaluate load transfer within the caving shield-lemniscate assembly to determine a complete profile of load mechanics among all shield components. This could be done by replacing all pin joints with instrumented load sensing pins.

It seems reasonable that all shields, because of the common pin-joint design,

will behave similarly to the shield tested in this study, and research efforts on other shields have suggested this to be true. However, future studies are needed to quantify the behavior of other shields so that more generalized conclusions can be drawn.

Finally, instrumented canopy-caving shield pins will be installed on active longwall shields underground to measure the participation of the caving shield in actual underground conditions. This is considered to be vital information with

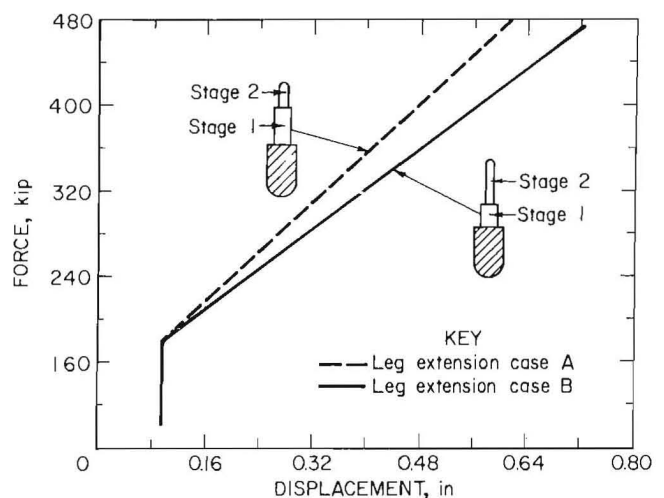


FIGURE 15.—Change in leg stiffness as a function of leg staging.

major impacts on shield design, since in the laboratory it was found that the caving shield does not participate fully

unless the canopy and base are fully constrained.

CONCLUSIONS

It is concluded from these initial studies that load transfer mechanics are important considerations in the design and optimization of shield supports. This research has provided additional insight toward a better understanding of shield responses to various canopy and base boundary (restraint) conditions and horizontal shield constraints through an investigation of load transfer. Future research efforts are needed to apply this information to investigate methods for improvement of support design and utilization.

Conclusions drawn from these research efforts are summarized as follows.

1. It is likely that the caving shield-lemniscate assembly is not participating fully in current shield designs because of translational freedom in the numerous pin joints.

2. Shields will respond differently to different boundary (restraint) conditions resulting from interaction with the strata. Generally, support resistance is increased for horizontally constrained canopy and base conditions and decreased for unconstrained conditions.

3. Both vertical and horizontal support resistance will be affected by the participation of the caving shield-lemniscate assembly. Horizontal support

resistance is most affected because of the larger horizontal (compared to vertical) stiffness of the caving shield-lemniscate assembly. When the canopy-caving shield joint is displaced horizontally toward the face, reactions developed in the caving shield-lemniscate assembly oppose leg reactions, thereby reducing overall shield capacity. Likewise, when this joint is displaced horizontally toward the gob, caving shield-lemniscate reactions act in the same direction as the leg reactions and thereby increase overall support capacity.

4. The caving shield-lemniscate assembly has virtually no capacity to resist vertical loading. This indicates the vertical response of the shield is dominated by the behavior of the leg cylinders. Load transfer implications are that vertical loads applied anywhere on the canopy surface must be transmitted by moment or shear through the canopy structure to the legs for transferral to the base.

5. The caving shield-lemniscate assembly has sufficient horizontal stiffness to provide stability against horizontal shield displacements. This suggests that the leg can be oriented in a vertical position to improve support efficiency and reduce unnecessary stressing of the support structure.

APPENDIX A.--DESCRIPTION OF MRS AND ITS CAPABILITIES

The mine roof simulator (MRS) is a large hydraulic press (see figure 3 of main text) designed to simulate the loading of full-scale underground mine roof supports. The MRS is unique in its ability to apply a vertical and a horizontal force or displacement simultaneously.

The vertical and horizontal axes can be programmed to operate in either force or displacement control. This capability permits tests, such as true friction-free controlled loading of shields, which cannot be accomplished in uniaxial test machines because the shield reacts a horizontal load to vertical roof convergence. Friction-free tests of this nature can be accomplished in the MRS by allowing the platen to float in the horizontal axis by commanding a zero horizontal load condition. Likewise, the MRS can apply controlled horizontal loading to a shield support, whereas uniaxial test machines can only apply vertical loading with no control over horizontal load reactions and no capability to provide a specified horizontal load to the structure. The controlled displacement capability allows determination of the stiffness of a structure, which is essential to understanding the load-displacement characteristics of the support.

The machine incorporates 20-ft-square platens with a 16-ft vertical opening to

enable full-scale testing of longwall roof support structure. Capacity of the simulator is 3 million lb of vertical force and 1.6 million lb of horizontal force with controlled displacement ranges of 24 in vertically and 16 in horizontally. Load and displacement control is provided in four ranges operating under a 12-bit analog-to-digital closed-loop control network, providing a load control capability of better than 0.1 kip (100 lb) and displacement control capability of better than 0.001 in. in the smallest load-displacement range.

Machine control and data acquisition are provided by a minicomputer. Eighty-eight channels of test article transducer conditioning are provided. Data acquisition is interfaced with the control network so machine behavior can be controlled by the response of the test-article transducer instrumentation. For example, tests can be terminated or held when strain values reach a designated level in specific areas of a support structure. High-speed data acquisition is available with a separate computer at a rate of 300 samples per second. An X-Y-Y recorder provides real-time plotting of three data channels and all data are stored on computer disks for subsequent processing and analysis.

APPENDIX B.--STIFFNESS TEST PROCEDURES AND RESULTS

The stiffnesses of the caving shield-lemniscate assembly and the full shield were determined from controlled displacement tests in the MRS in accordance with the analytical models previously described in the main test of this report. Tests were conducted and repeated at four different (shield) heights. These heights of 56, 68, 78, and 87.5 in were chosen to represent the operating range of the shield. Two displacement patterns were utilized as illustrated in figure B-1: one with a vertical displacement followed by a horizontal displacement, designated as VH, and the other with a horizontal displacement followed by a vertical displacement, designated as HV. All tests were conducted under full canopy and base contact without gob loading on the caving shield.

As indicated by equations 1 through 4 of the main text, stiffness coefficients K1 and K3 are determined from vertical displacements and coefficients K2 and K4 from horizontal displacements. As an example of this procedure, figure B-2 depicts full shield stiffness tests.

CAVING SHIELD-LEMNISCATE ASSEMBLY RESULTS

Caving shield-lemniscate assembly stiffnesses were accomplished by removing the canopy from the shield and attaching the canopy-caving shield joint to a fixture in the MRS. The base was also

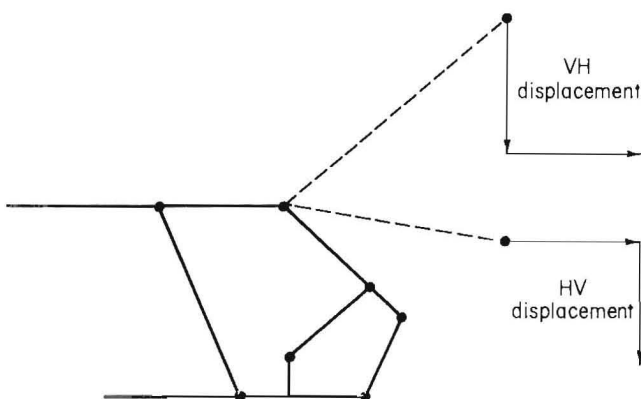
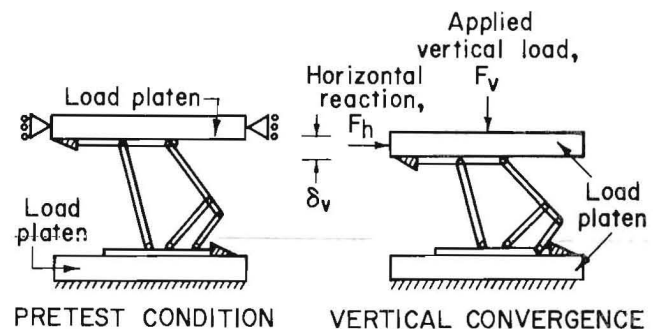


FIGURE B-1.--Displacement patterns for stiffness tests.

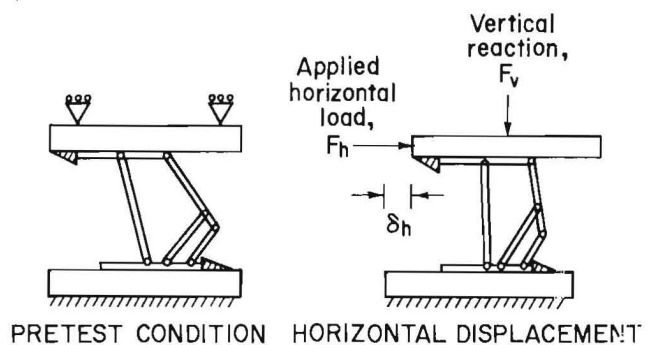
horizontally restrained to prevent slipping during horizontal displacements. To simulate boundary conditions imposed on this assembly by the leg cylinders, the base was also restrained vertically to prevent lifting of the base (as prevented by the leg in a full shield configuration). The test set up and constraints are shown in figure B-3. In addition, the canopy-caving shield connection was fitted with an instrumented vertical and horizontal load sensing pin to monitor load applied to the assembly. Horizontal pin translational freedom was removed from the assembly prior to the test to determine the true stiffness capability of the assembly. This was accomplished



$$F_v = K_1 \delta_v + K_2 \delta_h \rightarrow \delta_h = 0 \rightarrow F_v = K_1 \delta_v$$

$$F_h = K_3 \delta_v + K_4 \delta_h \rightarrow \delta_h = 0 \rightarrow F_h = K_3 \delta_v$$

A. VERTICAL DISPLACEMENT



$$F_v = K_1 \delta_v + K_2 \delta_h \rightarrow \delta_v = 0 \quad F_v = K_2 \delta_h$$

$$F_h = K_3 \delta_v + K_4 \delta_h \rightarrow \delta_v = 0 \quad F_h = K_4 \delta_h$$

B. HORIZONTAL DISPLACEMENT

FIGURE B-2.--Example of stiffness determinations in MRS.

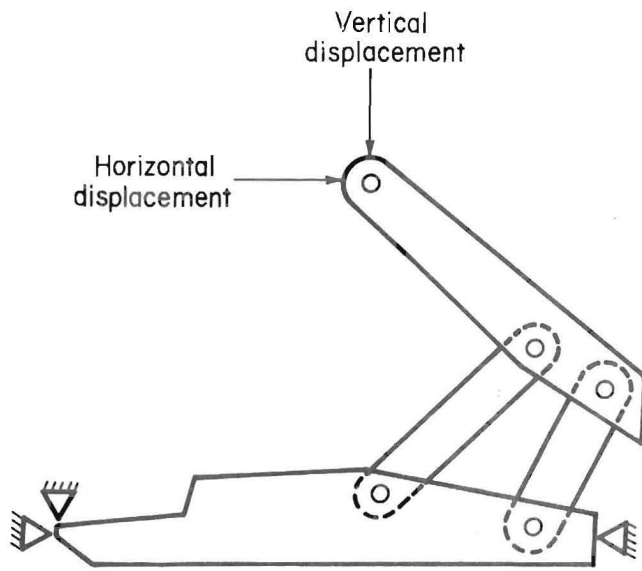


FIGURE B-3.—Caving shield-lemniscate assembly stiffness test conditions.

by horizontally displacing the canopy-caving shield joint until a horizontal force was registered in the load sensing pin.

An example of the load-displacement relationship for the caving shield-lemniscate assembly is shown in figure B-4. As seen in this figure, stiffness coefficients $K1_c$ and $K3_c$ are invariant (linear load-displacement response) throughout the vertical displacement controlled portion of the tests, while $K2_c$ and $K4_c$ exhibit more of a nonlinear response.

The results of the caving shield-lemniscate assembly stiffness tests for each of the four (shield) heights are documented in figures B-5 (VH tests) and B-6 (HV tests). In general, the results are as follows. For a vertical displacement with no horizontal displacement, no

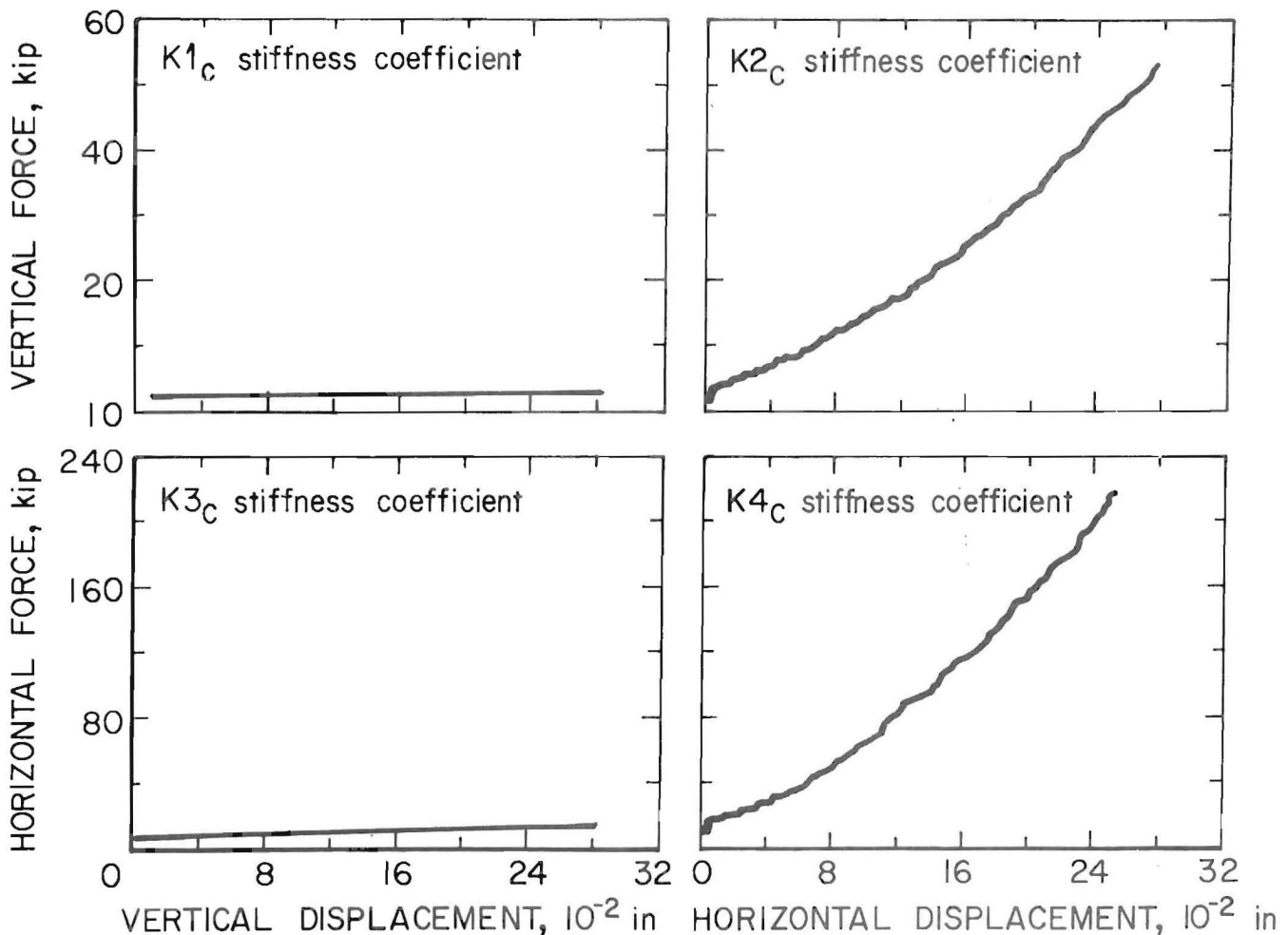


FIGURE B-4.—Example of load-displacement relationship for caving shield-lemniscate assembly.

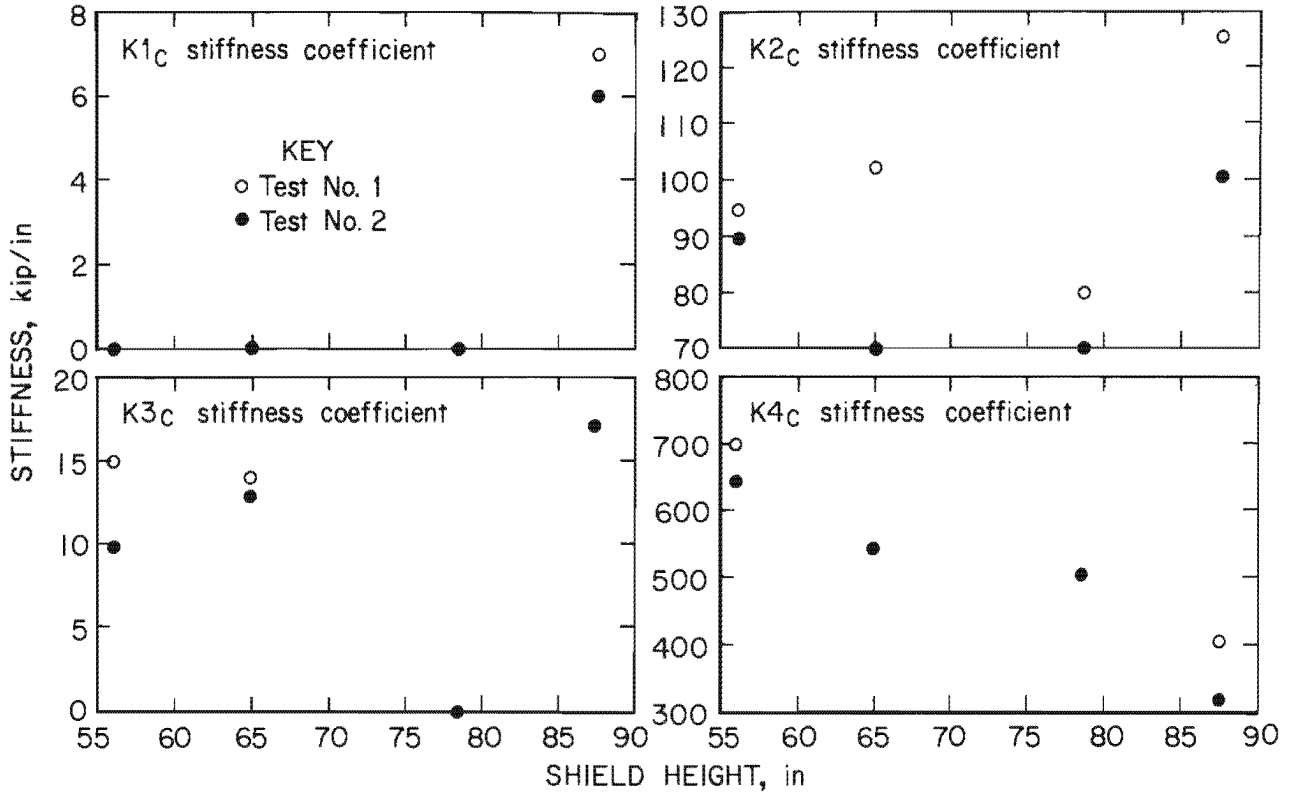


FIGURE B-5.-VH caving shield-lemniscate assembly test results.

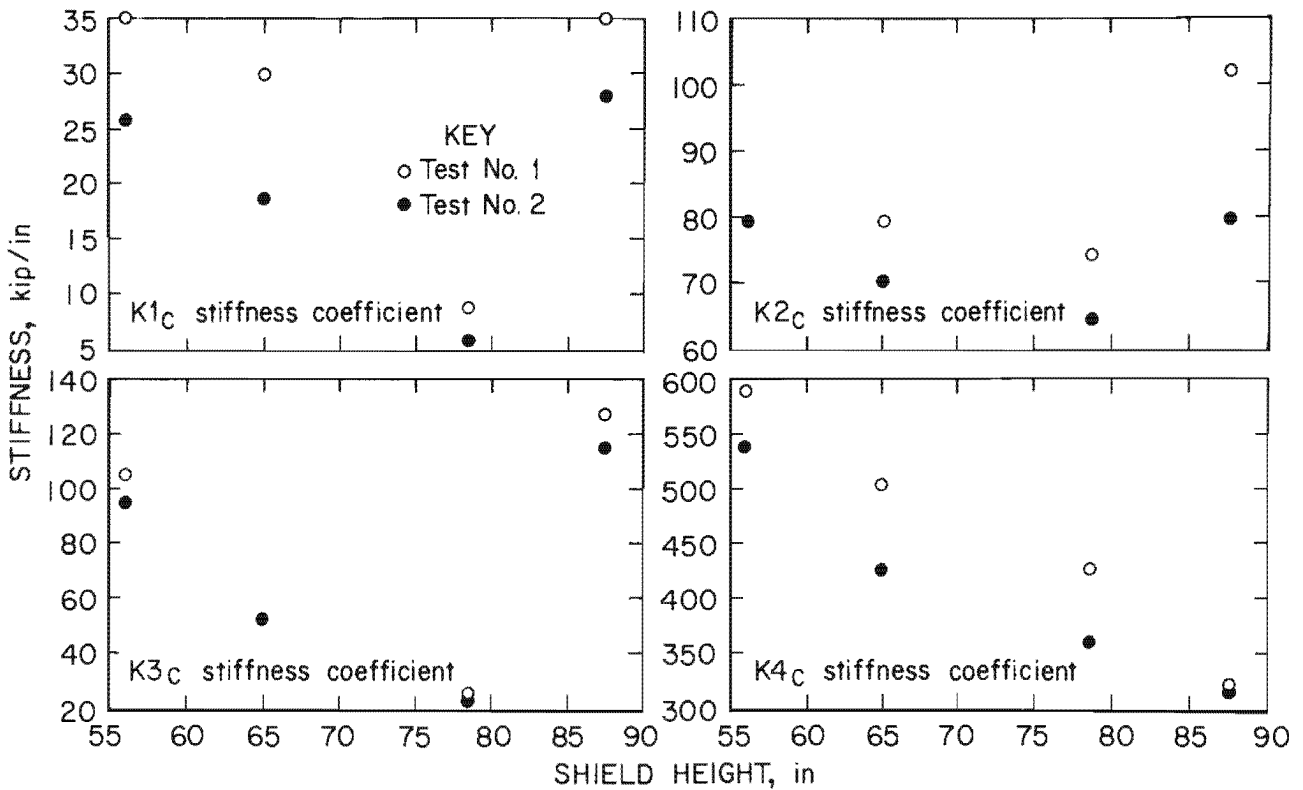


FIGURE B-6.-HV caving shield-lemniscate assembly test results.

vertical force resistance is generated by the assembly ($K1_c * V_c$ is zero), and the negative horizontal force resistance ($K3_c * V_c$) is insignificant throughout the range of heights examined. Superimposing the effects of a positive horizontal displacement, the additional forces generated are a small positive vertical component ($K2_c * H_c$) and a large negative horizontal ($K4_c * H_c$) resistant component. In comparison, for a positive horizontal displacement only, figure B-6 indicates that a small positive vertical resistance and a large negative horizontal resistance are generated. Again, superimposing a vertical displacement develops a small positive vertical

resistance ($K1_c * V_c$) and a somewhat larger negative horizontal resistance ($K3_c * H_c$).

FULL SHIELD RESULTS

Full shield stiffnesses were determined for full canopy and base contact conditions under horizontally constrained and unconstrained conditions prior to setting. The horizontally constrained condition was utilized to eliminate pin translational freedom in the numerous pin joints. A comparison of stiffnesses for the constrained and unconstrained conditions is illustrated in figures B-7 (VH tests) and B-8 (HV tests).

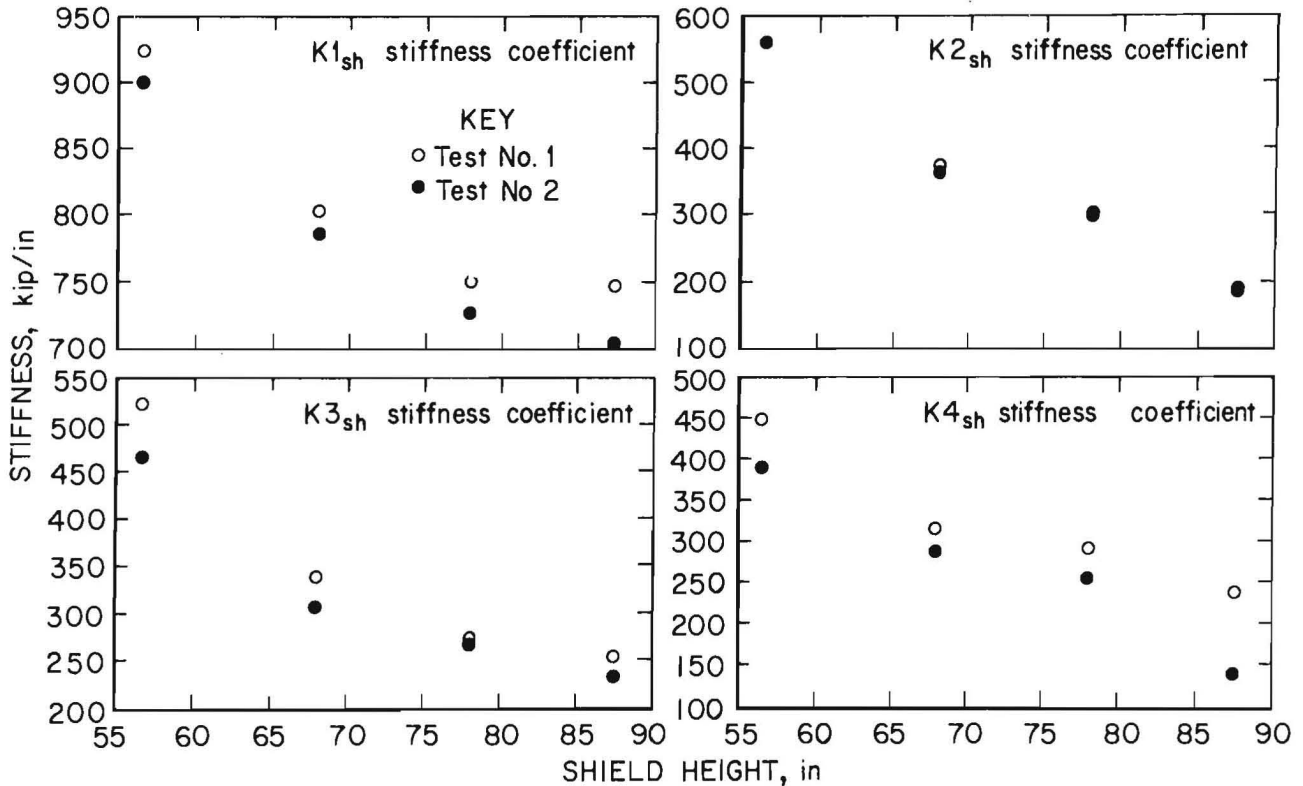


FIGURE B-7.—Unconstrained full shield stiffness results.

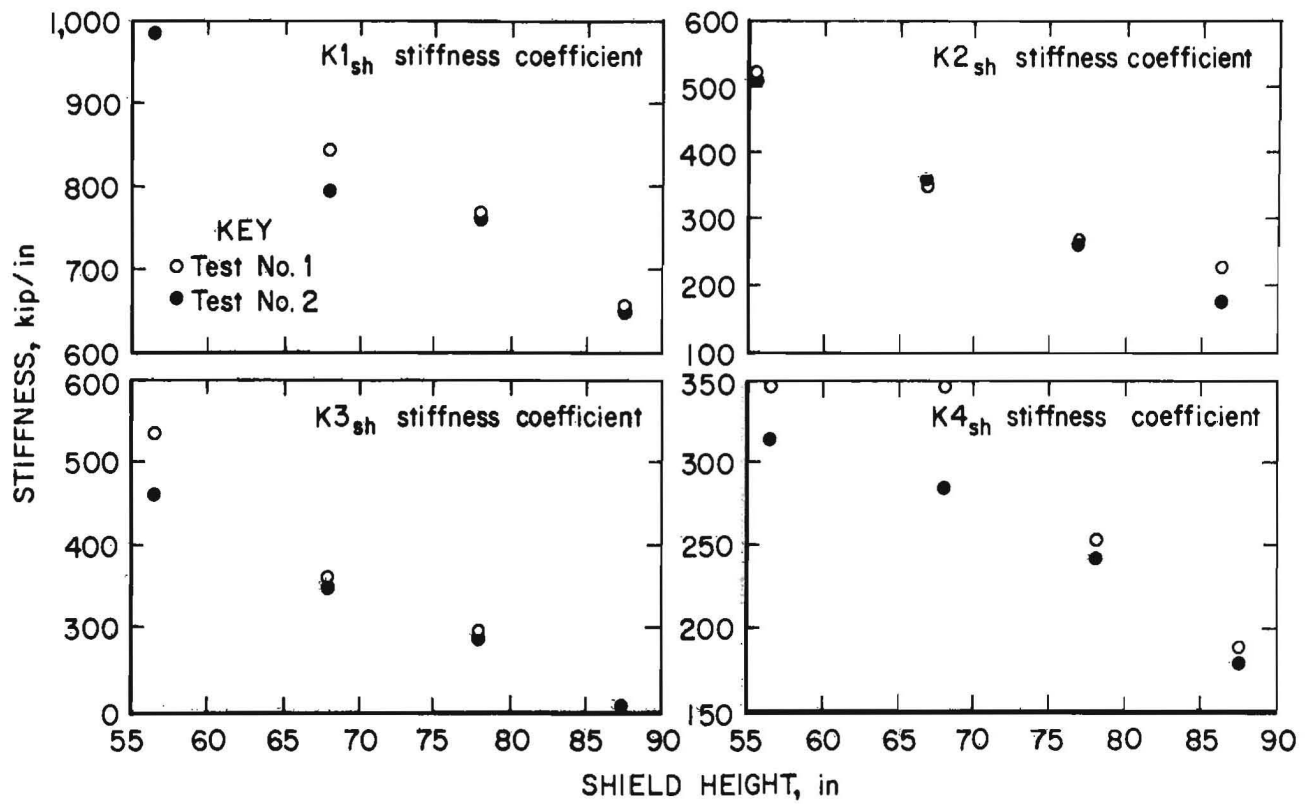


FIGURE B-8.—Constrained full shield stiffness results.

APPENDIX C.--SHIELD MECHANICS EQUILIBRIUM ANALYSIS

FRICTIONLESS CANOPY ANALYSIS

Reference is made to figures 8 and 9 of the main text. The figures depict applied loadings, restraints, and internal shield forces for negative (waste-to-face) canopy displacements relative to the base. For frictionless canopy conditions, HF_1 , HF_2 , and HF_3 would equal zero as there would be no external horizontal force acting upon the support.

From summation of forces at the leg joint (figure 9 of main text),

$$\begin{aligned} \Sigma F_x &= -HF_1 - L_h - HF_2 \\ &+ (HF_c - HF_3) = 0, \text{ and} \quad (C-1) \end{aligned}$$

$$\begin{aligned} HF_{sh} \text{ (External force acting on canopy)} \\ &= HF_1 + HF_2 + HF_3. \quad (C-2) \end{aligned}$$

Therefore, substituting equation C-2 into equation C-1,

$$\begin{aligned} \Sigma F_x &= -HF_{sh} - L_h + HF_c = 0, \\ HF_{sh} &= HF_c - L_h \text{ (as indicated in} \\ &\text{equation 8 of main text),} \\ \Sigma F_y &= -VH_1 + L_v - VF_2 \\ &- (VF_c + VF_3) = 0, \text{ and} \quad (C-3) \end{aligned}$$

$$\begin{aligned} VF_{sh} \text{ (external vertical force)} \\ &= VF_1 + VF_2 + VF_3. \quad (C-4) \end{aligned}$$

Therefore, substituting equation C-4 into equation C-3,

$$\begin{aligned} F_y &= -VF_{sh} + L_v - VF_c = 0, \text{ and} \\ VF_{sh} &= L_v - VF_c \text{ (as indicated in} \\ &\text{equation 9 of main text).} \end{aligned}$$

RESTRAINED CANOPY AND BASE

Reference is made to figure 10 of the main text. When the canopy is horizontally restrained, there is no horizontal movement of the canopy relative to the base. Hence, the caving shield-lemniscate assembly is subjected to vertical displacements only and because this assembly has little vertical stiffness ($VF_c = Kl_c * V_c$ and $HF_c = K_3 * V_c$ is small), the caving shield-lemniscate assembly does not contribute to overall shield capacity.

From summation of forces at the leg joint,

$$\begin{aligned} HF_{sh} &= HF_1 - HF_2 - HF_3 \\ &+ L_h = 0, \text{ and} \quad (C-5) \end{aligned}$$

$$HF_{sh} = HF_1 + HF_2 + HF_3. \quad (C-6)$$

Therefore, substituting equation C-6 into equation C-5,

$$\begin{aligned} HF_{sh} &= L_h, \\ \Sigma F_y &= VF_1 - L_v, \text{ and} \quad (C-7) \\ VF_{sh} &= VF_1. \quad (C-8) \end{aligned}$$

Therefore, substituting equation C-8 into equation C-7,

$$VF_{sh} = L_v.$$

FACE-TO-WASTE STRATA MOVEMENT

Reference is made to figures 11 and 12 of the main text. From summation of forces at the leg joint.

$$\begin{aligned} \Sigma F_x &= HF_1 - L_h + HF_2 \\ &- (HF_c - HF_3) = 0, \text{ and} \quad (C-9) \end{aligned}$$

$$HF_{sh} = HF_1 + HF_2 + HF_3, \quad (C-10)$$

Therefore, substituting equation C-10 into C-9,

$$HF_{sh} - L_h - HF_c = 0.$$

$HF_{sh} = L_h + HF_c$ as indicated by equation 10 of the main text,

$$\begin{aligned} \Sigma F_y = -VF_1 + L_v - VF_2 - VF_3 \\ + VF_c = 0, \text{ and} \end{aligned} \quad (C-11)$$

$$VF_{sh} = VF_1 + VF_2 + VF_3. \quad (C-12)$$

Therefore, substituting equation C-12 into equation C-11,

$$-V_{sh} + L_v + VF_c = 0, \text{ and}$$

$V_{sh} = L_v + VF_c$ as indicated by equation 11 of the main text.